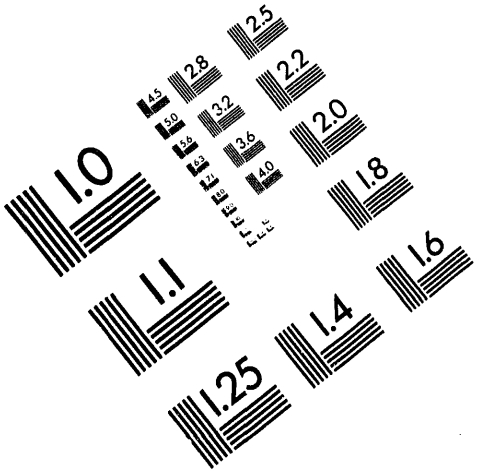

Association for Information and Image Management

1100 Wayne Avenue, Suite 1100
Silver Spring, Maryland 20910

301/587-8202

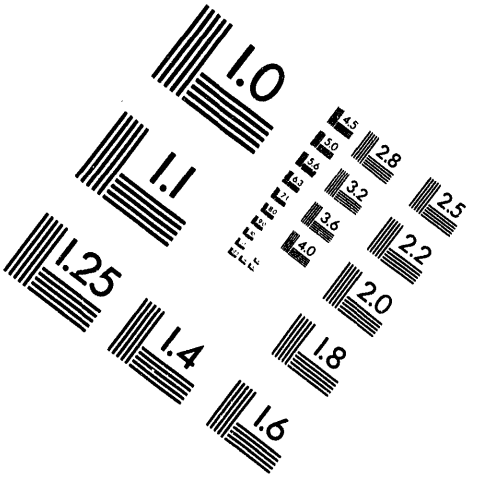

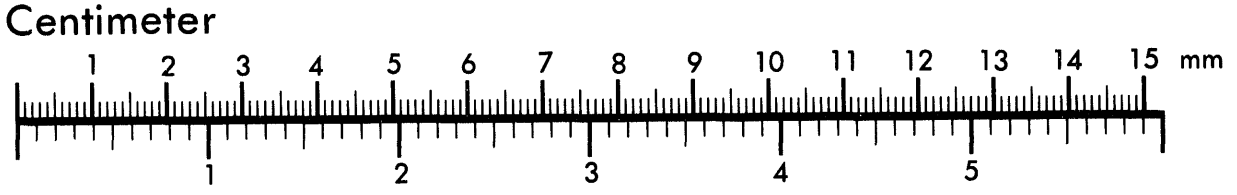

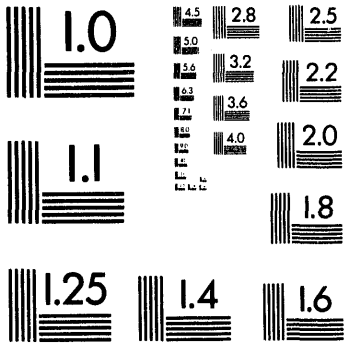

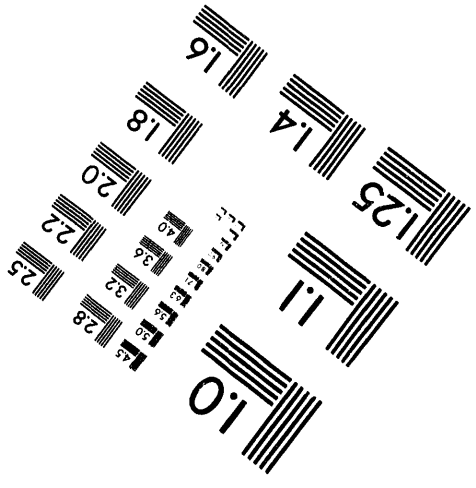

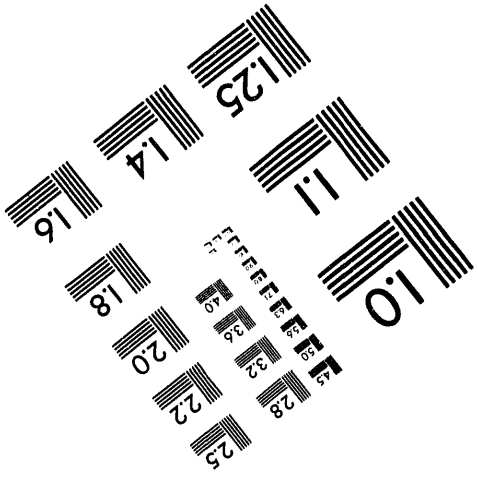

1 of 1

LA-UR- 94-2528

Conf-9406229--1

METASTABLE BCC PHASE FORMATION IN THE Nb-Cr-Ti SYSTEM

D. J. Thoma, *Los Alamos National Laboratory, Material Science and Technology Division, Mail Stop G770, Los Alamos, New Mexico 87545 USA*

J. H. Perepezko, *University of Wisconsin, Department of Materials Science and Engineering, 1509 University Avenue, Madison, Wisconsin 53706 USA*

Presented at the ISMANAM-94 Grenoble, France, June 27-July 1, 1994

To be published in Materials Science Form

DISCLAIMER

METASTABLE BCC PHASE FORMATION IN THE Nb-Cr-Ti SYSTEM

DAN J. THOMA[1] AND JOHN H. PEREPEZKO[2]

[1] Los Alamos National Laboratory, Materials Science and Technology Division,
Mail Stop G770, Los Alamos, New Mexico 87545 USA

[2] University of Wisconsin, Department of Materials Science and Engineering
1509 University Avenue, Madison, Wisconsin 53706 USA

Keywords: Nb-Cr-Ti, splat-quenching, liquid undercooling, extended solid solutions, metastable precursor phases

Abstract

Metastable disordered bcc phases have been formed from the melt in the Nb-Cr-Ti system where primary Laves phases would develop under equilibrium solidification conditions. Three vertical temperature-composition sections in the ternary system incorporating $NbCr_2$ were evaluated: the Nb-Cr binary, the $TiCr_2$-$NbCr_2$ isoplethal section, and the $NbCr_2$-Ti plethal section. In the rapid solidification of $NbCr_2$, metastable bcc phase formation was not observed, but deviations from $NbCr_2$ stoichiometry or alloying with Ti was found to promote bcc phase formation by decreasing the required liquid undercooling to reach the metastable bcc liquidus and solidus. The metastable phases were characterized through x-ray diffraction (XRD), and systematic deviations from Vegard's Rule have been defined in the three plethal sections. The metastable bcc phases decompose at temperatures >800°C to uniformly refined microstructures. As a result, novel microstructural tailoring schemes are possible through the metastable precursor microstructures.

Introduction

Alloys based upon $NbCr_2$ are being explored for high temperature structural applications [1-3] because of the high melting temperature (about 1730°C), reasonable oxidation resistance [4,5], appreciable creep resistance [4] and high temperature strength [6] of the ordered intermetallic compound. Although monolithic $NbCr_2$ exhibits low room temperature ductility and toughness [6-8], composite structures of the C15 Laves phase and a bcc phase have been shown to improve the low temperature toughness in $NbCr_2$-(Nb) [7], $NbCr_2$-(Cr) [3], and $(Nb,Ti)Cr_2$-(Nb,Ti) [8] alloys. In addition, the $NbCr_2$ phase exhibits a relatively wide single-phase homogeneity range with both (Nb) and (Cr) on either side of the compound in the binary system, and the Laves phase field broadens further in the ternary Nb-Cr-Ti system (Fig. 1a) [9].

The Nb-Cr phase diagram has been investigated recently to resolve conflicting phase boundary and invariant eutectic compositions under equilibrium conditions [10] and is shown in Fig. 1b along with the calculated T_0(bcc-liquid). Based upon the continuous T_0(bcc-liquid) between niobium and chromium, the formation of a continuous bcc solid solution appeared possible and was experimentally demonstrated with rapid solidification [11]. Since titanium exhibits a continuous bcc solution with both niobium and chromium in the respective binary equilibrium systems, the formation of continuous metastable bcc solid solutions in the Nb-Cr-Ti system also appeared to be possible. The objective of this study was to examine the formation of metastable bcc solid solutions in the ternary system by rapid solidification, as well as to explore the thermal stability of the metastable product in this high temperature system.

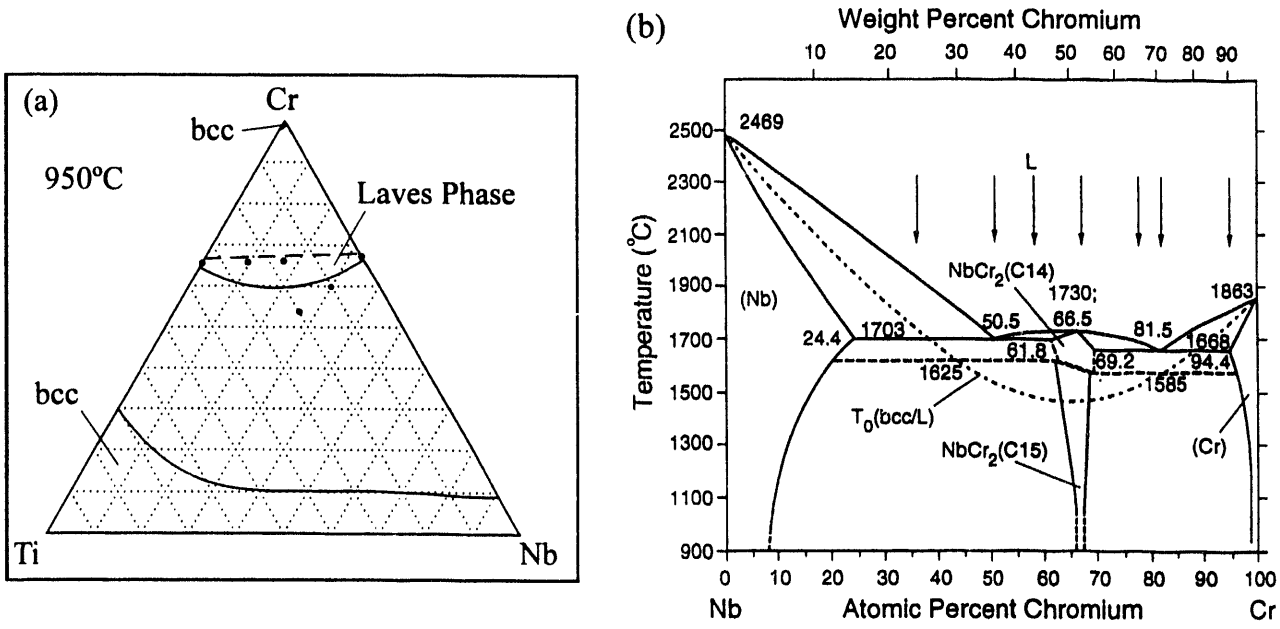

Figure 1 - Phase diagrams of the (a) ternary Nb-Cr-Ti system (in atomic %) [9], and (b) binary Nb-Cr system [11]. Dots and arrows indicate the nominal alloy compositions evaluated in this study.

Experimental Procedure

The rapid solidification technique of two-anvil splat-quenching was used on the twelve nominal alloy compositions illustrated in Figs. 1a and 1b. The splat-quenching process started with the levitation melting of a 60-100 mg piece of an arc-cast ingot in an evacuated (10^{-3} Pa) and purged Ar environment (~0.5 atm). The falling molten droplet was splat quenched between the two copper anvils at an estimated cooling rate of 10^5-10^8 K s^{-1} [12] in the resultant foil (~25-50 μm thick). The metal purities of the Nb, Cr, and Ti used for arc-melting were 99.8%, 99.99%, and 99.99%, respectively. After processing, alloy compositions were determined with elemental-standard-based energy-dispersive spectroscopy (EDS) and were close to the nominal compositions. X-Ray diffraction (XRD) with Cu Kα radiation was used to measure the lattice parameters. The machine accuracy was calibrated using Nb and Cr standards to within 0.02%, and typical precisions of the lattice parameter regressions were within ±0.001 Å.

Results

The XRD scans of the twelve splat-quenched alloys are shown in Figs. 2-4. The binary Nb-Cr alloys in Fig. 2 show only diffraction peaks for the metastable bcc phase in the niobium-rich and chromium-rich alloys. The alloy compositions close to $NbCr_2$ show diffraction peaks for the metastable bcc phase at the nominal composition which formed during rapid quenching. In addition, the patterns indicate diffraction peaks for the metastable high temperature C14 phase, the stable low temperature C15 Laves phase [10], and the equilibrium bcc phases. The splat-quenched sample at the $NbCr_2$ composition exhibits no bcc diffraction peaks.

The XRD traces of the splat-quenched alloys with 10 and 20 at.% Ti additions to $NbCr_2$ exhibited increasing amounts of the metastable bcc phase with respect to the Laves phase as the titanium content increased (Fig 3). Under equilibrium processing conditions, the Laves phases are the primary phases to develop from the melt, and some interdendritic bcc phases exist with lattice

parameters between 3.25 Å and 3.28 Å [13,14]. However, the lattice parameters of the bcc phases formed during splat-quenching are 3.0798 Å and 3.0956 Å for the 10 % and 20 % Ti alloys, respectively. Assuming Vegard's Rule along the $NbCr_2$-Ti plethal section, the bcc lattice parameter would increase from ~3.04 Å (for the metastable bcc phase at the $NbCr_2$ composition [11]) to 3.28 Å (for the metastable bcc phase at pure Ti [15]). The data clearly follows this trend, indicating a large amount of solute entrapment by the bcc phase during rapid solidification.

The XRD traces of the splat-quenched alloys along the isoplethal $TiCr_2$-$NbCr_2$ section are indicated in Fig. 4. Under equilibrium phase development solidification conditions, the bcc phase is the primary solidification product at the $TiCr_2$ composition. If negligible solid diffusion occurs in the solidifying bcc phase, the composition can vary from 80 at.%Cr (the first solid to freeze) to 40 at.% Cr (the final solid to freeze at the isomorph minimum)[15]. The resultant lattice parameter of the bcc phase would vary between 2.98 to 3.20 Å [15]. However, in splat-quenching, the bcc phase forms with lattice parameter of 3.0127 Å with minimal skewing. Lattice parameter vs. composition analysis in the Ti-Cr system shows that the lattice parameter at the composition of the splat should be ~3.03 Å [15]. Apparently, in the splat-quenching of the $TiCr_2$ composition alloy, a significant proportion of solidification occurred with solute entrapment approaching partitionless conditions since the lattice parameter is very close to that of the homogenized bcc phase.

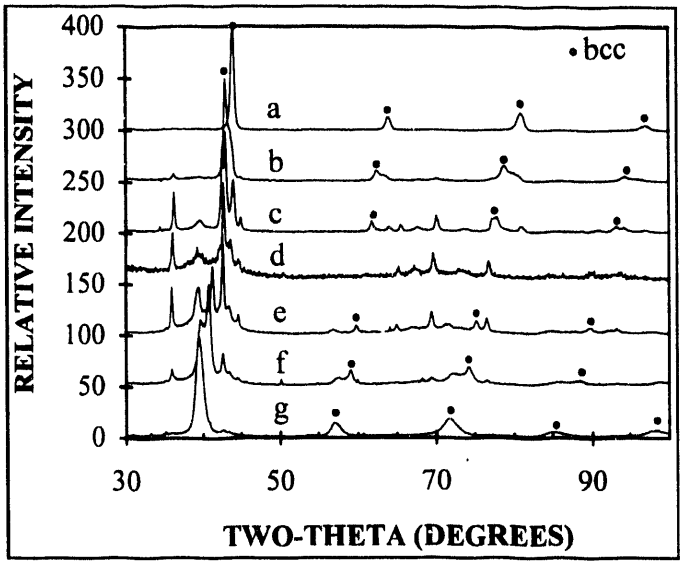

Figure 2 - XRD traces of splat-quenched Nb-Cr alloys for the nominal atomic per cent compositions of (a) 94% Cr, (b) 82% Cr, (c) 77% Cr, (d) 67% Cr, (e) 57% Cr, (f) 50% Cr and (g) 35% Cr.

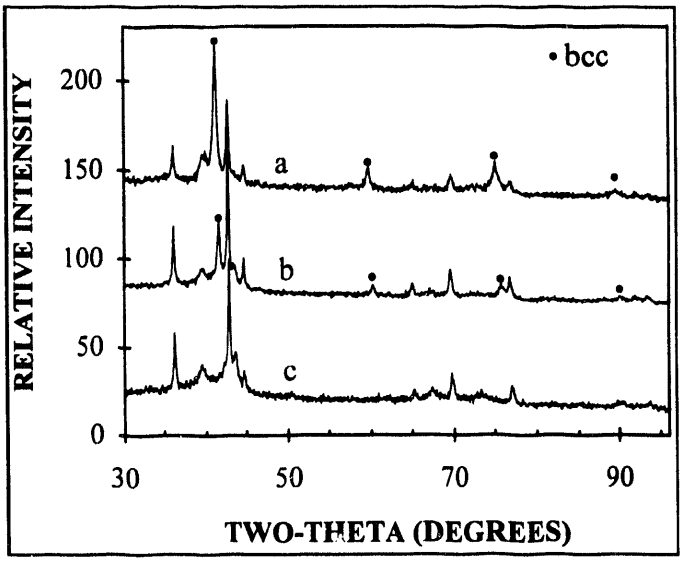

Figure 3 - XRD traces of splat-quenched alloys along the $NbCr_2$-Ti plethal section with the nominal atomic per cent compositions of (a) $NbCr_2$+10%Ti, (b) $NbCr_2$+20%Ti and (c) $NbCr_2$.

The $TiCr_2$-35wt.%$NbCr_2$ and $TiCr_2$-56wt.%$NbCr_2$ alloys form a primary Laves phase under equilibrium solidification conditions with no detectable bcc phases present in the XRD traces [14,16]. However, with splat-quenching the majority of the XRD traces consist of a bcc phase with some of the Laves phases present. The bcc phase lattice parameters for the splat-quenched $TiCr_2$-35wt.%$NbCr_2$ and $TiCr_2$-56wt.%$NbCr_2$ alloys are 3.0207 Å and 3.0130 Å, respectively. At the $TiCr_2$ composition, the lattice parameter of the bcc solid solution should be ~3.01 to 3.03 Å. At the $NbCr_2$ composition, the lattice parameter has been shown to be 3.04 Å [11]. Therefore, the ternary metastable bcc phase lattice parameter for the isoplethal alloys suggest an adherence to a ternary Vegard's Rule. Again, this

observation agrees with near partitionless solidification as suggested with the other bcc phases produced.

As the alloy compositions approach $NbCr_2$ from $TiCr_2$, the relative proportion of the bcc phase with respect to the Laves phases decreases. An etched cross-section of the splat-quenched $TiCr_2$-56wt.%$NbCr_2$ alloy is shown in Fig. 5(a) together with a schematic diagram of the microstructure in Fig. 5(b). The microstructure consists of a mottled columnar-type growth of the bcc phase emanating from one anvil side of the foil and growing into the middle of the splat. On the other anvil side, a faceted cellular/dendritic growth of the Laves phase is evident, and this primary Laves phase eventually was consumed by the typical bcc phase microstructure to the middle of the splat where impingement of the bcc growth fronts occurred. It is difficult to ascertain whether nucleation and growth of the metastable bcc phase occurred at the faceted Laves dendrites or whether the bcc phase merely grew faster around the Laves phase and consumed the development of the Laves phase. However, the occurrence of the Laves phase regions were not abundant, and the regions were less abundant in the $TiCr_2$-35wt.%$NbCr_2$ alloy.

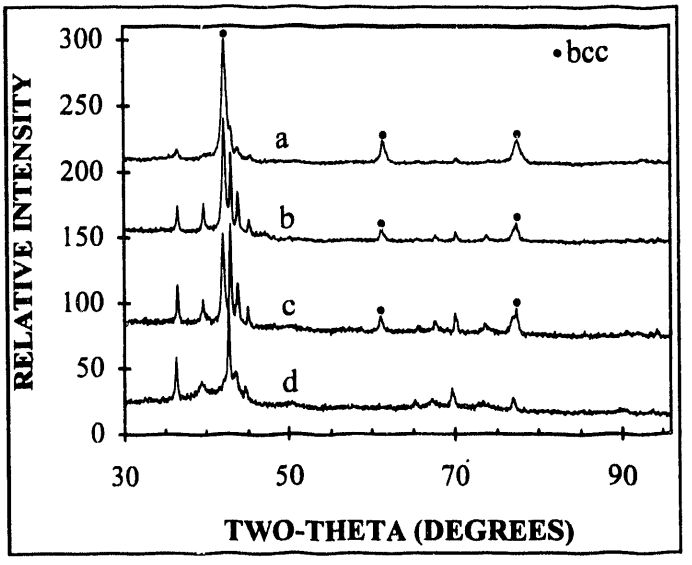

Figure 4 - XRD traces of splat-quenched alloys along the $NbCr_2$-$TiCr_2$ isoplethal sections with the nominal compositions of (a) $TiCr_2$, (b) $TiCr_2$-35wt.%$NbCr_2$, (c) $TiCr_2$-56wt.%$NbCr_2$ and (d) $NbCr_2$.

A proposed solidification pathway of the metastable bcc phase is given in Fig. 5(c). The metastable extensions of the bcc liquidus and solidus (dashed lines) across the isoplethal section is based upon the proposed $TiCr_2$-$NbCr_2$ isoplethal diagram [16], the existing binary diagram [11], and the low temperature ternary isotherm [9]. The alloy solidification pathway is shown to consist of an initial liquid undercooling (line 1) to some unknown temperature below the T_0 (dotted line). Upon recalescence, the initial solid formation approaches partitionless freezing as shown by the vertical lines (line 2). At the completion of recalescence, some solute partitioning may occur (line 3).

The lattice parameters from the splat-quenched samples are plotted as a function of alloy composition (as determined through EDS analysis) in Fig. 6. Also plotted in Fig. 6 is a ternary Vegard's Rule plane. Along the Nb-Cr binary, the lattice parameters indicate a positive deviation

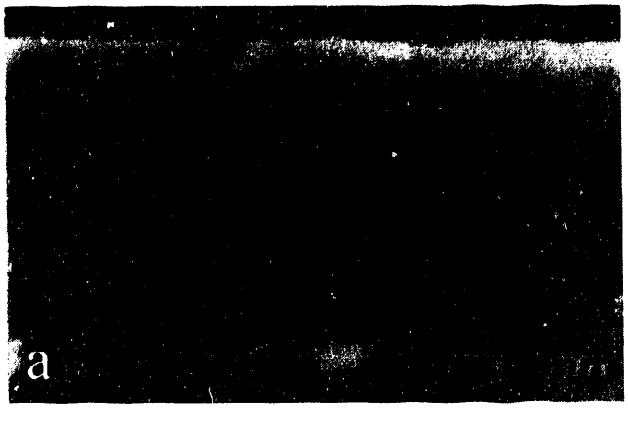

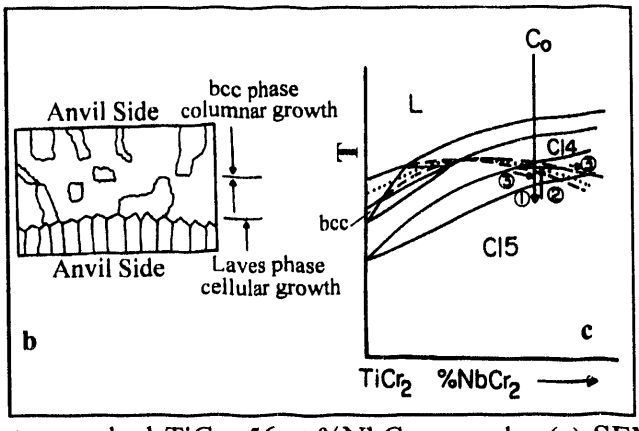

Figure 5 - Microstructural development in a splat-quenched $TiCr_2$-56wt.%$NbCr_2$ sample: (a) SEM micrograph, (b) schematic diagram of the microstructure, and (c) proposed solidification pathway.

from Vegard's Rule [11]. Between $TiCr_2$ and $NbCr_2$ the lattice parameters deviate from Vegard's Rule in a slightly negative manner. The data along the $NbCr_2$-Ti plethal section lies along the Vegard's Rule line. In general the lattice parameters closely follow the Vegard's Rule in ternary space, graphically illustrating the level of supersaturation obtained during splat-quenching.

After the metastable synthesis, the thermal stability of some of the splat-quenched alloys was investigated by differential thermal analysis (DTA) using heating rates of 15°C min^{-1}. The Nb-50%Cr, Nb-82%Cr, and $NbCr_2$+10%Ti alloys decomposed at 885, 930, and 800°C, respectively. XRD analyses after decomposition of the splats showed the expected coexistence of equilibrium C15 Laves and bcc structures [10,13]. A scanning electron micrograph (backscattered mode) of the decomposed $NbCr_2$+10%Ti alloy is shown in Fig. 7. The structure consists of dark matrix of $(Nb,Ti)Cr_2$ with isolated light dispersoids (~1 μm in size) of the (Nb,Ti) solid solution. The structures of the other two binary alloys also consisted of an intermetallic matrix with bcc dispersoids [11].

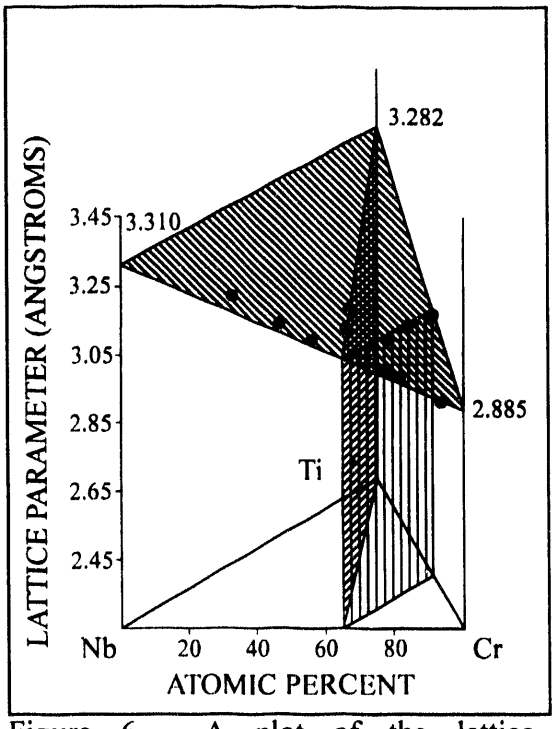

Figure 6 - A plot of the lattice parameters as a function of composition. The filled plane represents Vegard's Rule in ternary space.

Figure 7 - An SEM micrograph (back-scattered mode) of a splat-quenched and decomposed $NbCr_2$+10at.%Ti sample.

Discussion

During rapid solidification, a continuous metastable solid solution was formed over a large extent of the ternary Nb-Cr-Ti diagram. The nucleation and growth of the metastable bcc phase competed successfully over the ordered intermetallic Laves phase. The one alloy which did not display a retained bcc phase was at the stoichiometric $NbCr_2$ composition. An analysis of the extent of liquid undercooling required to promote metastable bcc phase formation [14] indicates that the temperature difference between the equilibrium liquidus and the metastable T_0(bcc-liquid) is greatest at the $NbCr_2$ composition ($T_0=0.12T_m$). Therefore, deviations from $NbCr_2$ stoichiometry or alloying with Ti promote bcc phase formation by decreasing the required liquid undercooling to reach the metastable T_0(bcc-liquid).

The continuous metastable solid solution formation can be attributed in part to Hume-Rothery rules for solid solubility. The normalized difference between the atomic radii of the metallic atoms is less than 15%: Nb and Cr is 13.8%; Ti and Cr is 13.1%; and Nb and Ti is 0.4%. In addition, the elements have the same crystal structure at high temperatures (bcc) and display similar electronegativities. Moreover, the measured bcc lattice parameters show only a slight positive deviation with respect to Vegard's Rule along the Nb-Cr binary section which may be associated with the tendency for a positive heat of mixing [11]. In the analogous Ti-Cr system [15] a similar behavior is observed along with an indication of a lattice parameter decrease near $TiCr_2$,

suggesting that a localized atomic interaction may be operative at the intermetallic composition. The negative deviation of the bcc lattice parameter with respect to Vegard's Rule is consistent along the $TiCr_2$-$NbCr_2$ isopleth.

The metastable bcc solid solutions are relatively stable, with decompositions during continuous heating occurring at temperature close to 60% of T_0(bcc-liquid). After decomposition of the splat-quenched metastable bcc solution to the equilibrium two-phase alloys, the resultant microstructures are dual-phase alloys with isolated bcc dispersoids in a Laves phase matrix. The decomposition of a metastable precursor bcc phase produced by rapid solidification contrasts with other *in situ* multiphase microstructure formation techniques (such as directional solidification or precipitation) in that the volume fractions of the phases can be designed to specific amounts. Therefore, considering the potential of $NbCr_2$ as a candidate high temperature structural material, particularly in composite form, an effective microstructural tailoring scheme to produce controlled multiphase microstructure of $NbCr_2$-based materials has been demonstrated with liquid undercoolings during rapid solidification processing.

Conclusions

Three main points are evident with the splat-quenching of Nb-Cr-Ti alloys.

(1) An extended metastable bcc solid solution can be produced over most of the ternary diagram, even where the Laves phase is the primary phase to form during equilibrium solidification.

(2) Deviations from $NbCr_2$ stoichiometry or alloying with Ti promote bcc phase formation by decreasing the required liquid undercooling to reach the metastable bcc liquidus and solidus.

(3) Decomposition of the metastable bcc precursor phase offers an effective technique to prepare uniformly refined $NbCr_2$-based microstructures.

Acknowledgments

This work was supported by DARPA, grant ARO-DAAL-03090-G-0183.

References

1. R.L. Fleischer and R.J. Zabala, *Metall. Trans. A*, **21** (1990) 2149.
2. G. E. Vignoul, J.M. Sanchez and J.K. Tien, *MRS Symp. Proc.*, **213** (1991) 739.
3. M. Takeyama and C.T. Liu, *Mater. Sci Eng. A*, **132** (1991) 61.
4. D.L. Anton and D.M. Shah, *MRS Symp. Proc.*, **213** (1991) 733.
5. H.J. Goldschmidt and J.A. Brand, *J. Less-Common Met.*, **3** (1961) 44.
6. R.L. Fleischer, *MRS Symp. Proc.*, **133** (1989) 305.
7. D.L. Anton and D.M. Shah, *MRS Symp. Proc.*, **194** (1990) 45.
8. D.L. Davidson, K.S. Chan and D.L. Anton, *AFOSR Report # F49620-92-C-0022,* (1994).
9. D.J. Thoma and J.H. Perepezko, in "Experimental Methods of Phase Diagram Determination", J.E. Morral, R.S. Schiffman and S.M. Merchant, eds. (TMS, Warrendale, PA) (1994) 45.
10. D.J. Thoma and J.H. Perepezko, *Mater. Sci. Eng. A*, **156** (1992) 97.
11. D.J. Thoma, J.H. Perepezko, D.H. Plantz and R.B. Schwarz, *Mater. Sci. Eng. A*, **179/180** (1994) 176.
12. P. Predicki, A.W. Mullendore and N.J. Grant, *Trans. Metall. Soc. AIME*, **223** (1965) 233.
13. D.J. Thoma and J.H. Perepezko, *MRS Symp. Proc.*, **194** (1990) 105.
14. D.J. Thoma, *Ph.D. Thesis*, University of Wisconsin-Madison, (1992).
15. F.B. Cuff, N.J. Grant, and C.F. Floe, *AIME Trans.*, **194** (1952) 848.
16. I.I. Kornilov, K.I. Shadhove, P.B. Budgerg, and N.A. Nedumov, *Dokl. Chem. Proc. Acad. Sci. USSR*, **149** (1963) 362.

DATE
FILMED
10/3/94
END